HIGH-SPEED TOMOGRAPHIC SPECTROMETRY OF A PLASMA

V. A. Zhovtyanskii

UDC 535.853:543.48.08

An example is presented of a method for simultaneously measuring the spatial and spectral characteristics of radiation in the diagnostics of a pulsed plasma.

Tomographic spectrometry arose as a trend in optical plasma diagnostics because it is necessary to provide local spatial diagnostic measurements of the contours of spectral lines which are radiated in pulsed processes. As a whole, tomographic spectrometry can totally recreate distribution of the spectral radiation capability of the plasma volume. The experimental procedure presumes that measurements (integrated along the line of sight) are made of the spectral radiation intensities of the layer from various directions. In the simplest case of an axisymmetric plasma it is sufficient to make measurements (usually on the order of ten) only along various chords [1]. If there are no indications of symmetry, then multiaspect measurements must be made [2], in which these observations along the chords are repeated many times from various directions (usually no more than ten).

A further transition to intrinsic radiation methods occurs from reducing the resultant experimental data with numerical tomography methods [2]. In the case of axisymmetric radiation sources a very simple Abel rotation method is also used: either a graphic method [3] or numerical method from tabulated coefficients (see [4], for example).

Here we limit ourselves to problems of selecting the initial experimental information. The crucial problem is to choose the type of spectral apparatus and cameras, and also the organization of their interaction. because the obvious solution, sequential measurement along each of the chords in various spectral intervals with a single monochromator with a radiation sensor at the output [5-7] is hardly productive and requires repeating the investigated phenomena over a long measurement procedure.

Earlier, in order to accelerate purely tomographic or purely spectral measurements of pulsed processes, a series of separate photosensors were often used along a number of observation chords or required spectral intervals (see [8], for example). However in the case of tomographic spectrometry, this approach is accompanied by a huge amount of equipment, even more so because a multichannel data-recording system is required.

The best alternative is to use a stigmatic spectrograph, in which the required plasma volume is focused at the input slit [9]. The information in the focal plane at the output is read using an image recorder: a charge-coupling array, lines of which record the spectral intensity distribution of integral radiation along one of the chords; a transition from line to line corresponds to a transition from chord to chord. We note that the same equipment can also be used in measuring multiple aspects, if fiber optics can be used to illuminate various sections of the input slit with radiation which is selected in accordance with various directions of observation [2]. Nonetheless, this method is rarely used. One reason is the relatively small transmissivity of stigmatic spectral devices. There are also time constraints related to reading the information from the output from the charge-coupling array.

Naturally traditional high-speed photographic methods can be used to record images [2, 10] in tomographic spectroscopy. However, these methods, as in current Physical experimental practice as a whole, have been replaced by modern scanning photosensors with an electrical output, which first of all provide a much higher time resolution an sensitivity, and also a higher information-processing efficiency. In recent years integral linear and matrix solid-state imaging sensors have been widely used; the most promising are the already mentioned charge-coupling devices and charge injection devices [11]. Also, dissectors – vacuum electronic devices such as used for TV transmission tubes, which do not have a charge-accumulation effect, have not lost their value as high-speed image sensors [12, 13].

T. G. Shevchenko Kiev State University. Translated from Inzhenerno-Fizicheskii Zhurnal, Vol. 62, No. 5, pp. 758-764, May, 1992. Original article submitted November 12, 1991.

1062-0125/92/6205-0545$12.50

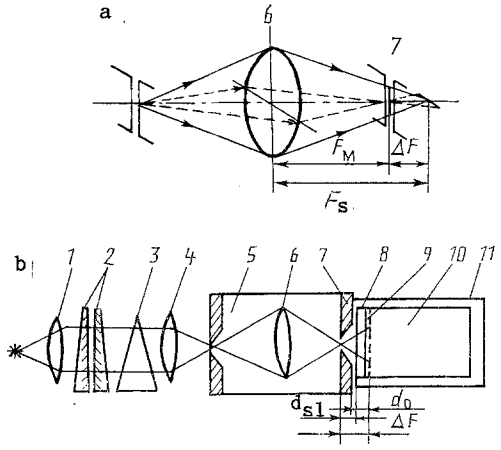

Fig. 1. Tomographic spectrometer: a) ray path; b) design: 1) collimator; 2) Fabry–Perot interferometer; 3) Dove [Delabourne] prism; 4) objective; 5) MDR-12 monochromator; 6) monochromator optical system (shown schematically); 7) output slit; 8) dissector window; 9) photocathode; 10) DI-14 dissector; 11) housing for dissector unit.

The information capacity of each of these sensor types (200 elements of resolution for the simplest dissectors to 10^4 for the most modern linear charge-coupling devices) is more than required in terms of spatial resolution elements in the case of tomographic investigations of an axisymmetric plasma (around 20 elements per image diameter). This makes it possible to make measurements not only of the total light or – if a spectral device is used – at a fixed wavelength, but also to make polychromatic measurements with a high spectral resolution. The latter possibility is realized by an original tomographic spectrometric method, in which the spectral sensor is a Fabry–Perot interferometer, which is hybridized with a wide-aperture diffraction monochromater [14]. This method has a series of substantial advantages. Here the source image at the output of the monochromator is modulated by a system of interference bands, each of which contains information on the shape of the spectral line emitted which is produced by the monochromator and which is irradiated along the corresponding chord of the plasma source. A feature of this method is the use of an astigmatic monochromator (Fig. 1), which first removes limitations on its transmissivity and second substantially simplifies the optical design of the instrument as a whole. Actually, in this monochromator, the image of the spectral line itself (which lies in the meridional plane, which coincides with the plane of the output slit of the spectral device) and the image of the interference bands which modulate the line (these bands lie in the saggital plane) have an astigmatic difference ΔF along the optical axis. For the rather widely used wide-aperture, small-size MDR-12 monochromator, $\Delta F \approx 15$ mm, which makes it possible to collocate the dissector photocathode, which is pointed to the inner surface of its output window, directly with the localization plane of the interference bands. As a result, it is possible to build a small wide-aperture tomographic spectrometer which provides high temporal and spectral resolution.

Calculated distortions of spectral line shapes from measurements made with dissector instruments as a function of the apparatus band width [15] can be used to estimate the number of resolution elements required in polychromatic measurements. From these measurements it follows that for satisfactory measurement accuracy. the apparatus band width should not exceed 1/4 the width of the spectral line shape at half maximum; in other words, 4 resolution elements are sufficient to measure the spectral line shape. On the whole. If a range of spectral line shapes must be measured, there should a total of 10-20 resolution elements along one chord. Thus, the number of chords along which line shapes are read usually is no more than ten. which leads to the conclusion that in this regard dissectors and solid-state imaging sensors also satisfy the requirements of tomographic spectrometry.

In processing spectrometer output records [14] to compute local intensities, it is only necessary to recall that the abscissa of each imaging element contains not only the spatial coordinate, but also the spectral characteristic. Naturally, the Fabry–Perot interferometer can be excluded as an optical instrument; in this case the spectrometer remains a convenient instrument for high-speed measurements of the radial profiles of spectral line radiation.

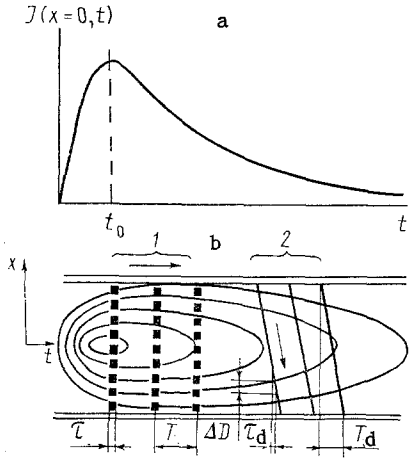

Fig. 2. Example of a time-dependent measurement of the intensity of plasma radiation J (x = 0, t) (a) and a schematic of its high-speed photoscan image (b); the closed curves are lines of equal intensity; 1) the group of time selections if a charge-coupling sensors are used; 2) if a dissector is used; the arrows show the scanning direction.

A series of other metrological characteristics of a high-speed tomographic spectrometer are also determined to a large degree by use of an image sensor. It should be noted that the solid-state imaging sensors have a small size, a low level of control voltages, a high information content, and are rather "technologically effective" from the standpoint of automating the measurements in pulsed processes. In regard to these parameters, dissectors are better than solid-state imaging sensors. Moreover, in the 70's and 80's it was the opinion that they were not promising because of significant light losses, as it was then assumed. As we will show, that assertion is limited in regard to the technology of high-speed tomographic spectrometry. To do this, we consider various types of images from each of these instruments. In spite of the fact that both types of imaging detectors are comparable to scanning instruments [16], there is a significant difference between them from the standpoint of reading the images. Figure 2 shows a schematic representation of the procedure for measuring the radial distribution of the radiation intensity of a pulsed axisymmetric radiation source in a discharge tube using both a solid-state imaging sensor and a dissector. Actually, we are talking about measuring the values of a two-dimensional intensity function J(x, t), where t is the time and x is the distance from the chord to the tube axis along which the observation is made (the spatial coordinate).

The linear type of solid-state imaging sensor is essentially a combination of N separate, small integrating photodetectors, each of which records the radiation intensity at a fixed point x_n, the location of the n-th photodetector (see 1 in Fig. 2b):

$$u(t) = \begin{cases} a \int_0^t J(x_n, t)\, d\tau \quad \text{for } 0 \leqslant t \leqslant \tau_{ss}, \\ a \int_0^{\tau_T} J(x_n, t)\, d\tau \quad \text{for } t > \tau_{ss}. \end{cases}$$

Here the duration of each separate measurement sample τ_{ss} and the interval between them T_{ss} is determined primarily by the duration and the repetition period of the strobe pulses, which directly control the choice of the solid-state imaging sensor. The value of τ_{ss} usually is chosen small enough so that each element of the solid-state imaging sensor actually measures almost instantaneous values of the radiation along a fixed chord with a time interval T_{ss}: $J(x_n, t)$, $J(x_n, t + T_{ss}), \ldots, J(x_n, t + mT_{ss})$.

The dissector forms an electronic image, an analog of the spatial distribution of the radiation intensity at its input (in this case from a discharge tube), which is scanned n the perpendicular direction (see 2 in Fig. 2b) with a selecting aperture with an electronic multiplier located behind it. Thus. the frequency spectrum of the dissector output signal reflects the spatial structure of the radiation source, with a consideration of the scanning rate of the image. Here the transformation takes place [16]

$$i(t) = bJ(\hat{x}(t),\ t),$$

where b is a proportionality coefficient determined mainly by the sensitivity and

$$\hat{x}(t) = \int_0^t v dt$$

is the running coordinate of the scanning trajectory. In the approximation described here, the scanning rate v is usually constant. This transformation is performed on the length of a direct path of the dissector scan in the interval $0 \leq t \leq T_d$. The effective duration of the measurement sample is determined by the scanning rate of the instrument curve ΔD of the dissector. which is reduced to the plane of the image (2 in Fig. 2b)

$$\tau_d = \Delta D/v.$$

Often investigators try to minimize the duration of the sweep T_d of the dissector to the value τ_d, which is characteristic of a sampling in a solid-state imaging sensor in studying continuous processes. Actually, however, "instantaneous" scanning of the spatial profile of the radiation is inefficient. because of the insignificance of the light energy picked up by the dissector during the read time, which naturally limits its sensitivity. It is actually necessary to compare the values of τ_{ss} and τ_d (see Fig. 2). But the fact that the samplings of the measurements relative to the spatial structure of the investigated object are not fixed simultaneously, but sequentially in time in the case of the solid-state imaging sensor, makes it necessary to consider the numerical tomography in the corresponding procedure.

A very substantial problem is the ratio of the output signal levels and the sensitivity of various photodetectors of the types in question. When a light flux J is recorded, the signal outputs from a dissector U_d and a solid-state imaging sensor U_{ss} are

$$U_d = iR = J\varkappa_d S_d kR; \tag{1}$$

and

$$U_{ss} = Q/C_{ss} = J\varkappa_{ss} S_{ss}\tau_{ss}/C_{ss}. \tag{2}$$

We note that the absolute photosensitivities of dissectors [17] and solid-state imaging sensors [18, 19] are close to each other.

When the ratios of the signal output levels of dissectors and solid-state imaging sensors in pulsed measurements are determined explicitly, the differences in the features in recording the radiation by each of these sensors should be considered. Here we note that performing tomographic measurements in pulsed process requires recording a series of samples of transverse observations of the plasma volume with a discretization period

$$T = 1/(2F_u).$$

In a solid-state imaging sensor, parallel signals in all cells are integrated over the sampling time τ_{ss}; the corresponding sampling duration to make the measurement error no worse than 1% should be $\tau_{ss} \sim 0.1 \cdot T$ [20]. The same level of measurement error by a dissector, which sequentially records instantaneous signal values is attained for $\tau_d \sim 0.01 \cdot T$ [20]. Thus, the process of scanning the transverse profile of the investigated object by a dissector should occupy practically the whole interval T_d.

The value of R in Eq. [1] is chosen to exclude substantial dynamic distortions the dissector output signal due to the "stretching" of the signal shape during scanning. Under rather rigid assumption, it can be formulated as

$$R \sim \tau_d/C_d.$$

In practice. however, the value of R can be much larger, due to the fact that the dissector is a current generator in relation to the output signal. Thus, under the most rigid assumptions on the dissector, by sequential substitutions into (1) and (2), and also by assuming that $\varkappa_d = \varkappa_{ss}$ and $S_d = S_{ss}$, we obtain the following expression for the ratio of the output signals from both types of sensors:

$$U_d/U_{ss} \sim 0.1 kC_{ss}/C_d.$$

From this it follows that, based on output signal level, the dissector has an advantage over the solid-state imaging sensor (here C_d = 10 pF is the output capacitance of the dissector and k ~ 10^6 [12]; C_{ss} ~ 0.1 pF for a charge-coupling device: and C_{ss} >> 0.1 pF for a charge-injection device [11, p. 49]).

In order to increase the sensitivity of image sensors with the use of a solid-state imaging sensor, the latter is often connected with an image converter tube which acts as an image preamplifier [21 (p. 43), 22, 23]. Dissectors, however, are significantly inferior to solid-state imaging sensors with respect to control voltage level, and dissectors and systems with charge-coupling devices and image converter tubes are inferior to solid-state imaging sensors themselves in weight and size characteristics. However, the last factors are not deciding ones under laboratory measurement conditions.

The intrinsic noise level for the better solid-state imaging sensors lies at the level for recording tens of electrons per element of structure [18, 24]. It can be shown that under typical sweep duration T = 1 μsec, which is sufficient for most plasma investigations, the noise is less than 1 electron per spatial resolution element, even for an outdated LI-602 dissector [12]. Consequently, on the hole, the dissector has the advantage in sensitivity, as characterized by the signal/noise ratio. We note that, in spite of widespread opinion, actual tomographic instruments using dissectors [14] are not inferior in time resolution to instruments based on solid-state imaging sensors. Actually, for T = 1 μsec and for L = 200 scanning elements, the time resolution is τ_d ~ T/L = 5 nsec.

Both dissectors and the best of the modern solid-state imaging sensors have a rather large dynamic range (on the level of 10^4-10^5).

Dissector-based recorders [12, 14, 25-27] were used to investigate free heated arc Plasmas and pulsed electrical arc plasmas with respect to the intensities and shapes of the spectral lines Ar I, Ar II, He I, He II [12, 28-30], and Cu I [14]. Laser absorption spectrometry methods have also been used [31].

Primarily electromagnetic dissectors [32-25] have been used in foreign developments for a similar purpose. In particular, they were used for survey observations of radiation spectra [32, 33] and for measuring the shapes of spectral lines [34]. An example of the use of an electrostatic dissector CBS-1147 (USA) with a deflectron deflection system has been presented [36].

Thus significant interest remains in using dissectors in tomographic spectrometry. Their best use is for conducting a cycle of measurements over a single event of an investigated pulsed process.

NOTATION

F_M and F_S – focal lengths of the monochromator in the meridional and saggital planes; ΔF – astigmatic difference; d_{sl} – thickness of the slit wall of the monochromator; d_0 – thickness of the input window of the dissector; a and b – proportionality coefficients; τ_{ss} and τ_d – durations of recording a measurement sample of radiation with a solid-state imaging sensor and with a dissector, respectively; T_{ss} and T_d – interval between samples when using a solid-state imaging sensor and with a dissector, respectively; x and t – spatial and time coordinates; $\hat{x}$ – running coordinate for the scanning trajectory; v – scanning rate; J – radiation intensity; u and U – output voltages of the radiation sensor; ΔD – width of the instrument curve of the dissector; i, k, R – collector current, gain, and resistance of the load resistor, respectively, for a dissector; S_d and S_{ss} – the area of the collimating aperture of a dissector and the collimating element of a charge-coupling sensor; $\varkappa$ – photosensitivity; Q – charge on an element of a charge-coupling sensor; F_u – upper frequency in the spectrum of the process under investigation.

LITERATURE CITED

1. M. I. Pergament, The Physics and Application of Plasma Accelerators [in Russian], Minsk (1974), pp. 261-288.
2. T. S. Mel'nikova and V. V. Pikalov, Izv. Siberian Otd. Akad. Nauk, Ser. Tekh Nauk, **11**, No. 3, 60-68 (1987).
3. N. G. Kolesnikvo, L. T. Lar'kina, and V. S. Éngel'sht, "Graphical method for making the Abel transformation." Deposition in the All-Union Institute of Scientific and Technical Information (VINITI), No. 313-75. Izv. Akad. Nauk. Kirgiz. (1975),
4. K. Bockasten, J. Opt. Soc. Am., **51**, No. 9, 943-947 (1961).
5. Yu. I. Chutov and V. A. Zhovtyanskii, Prib. Tekh. Éksp., No. 4, 225-226 (1977).
6. B. Cheminat, R. Gadaud, and P. Andanson, J. Phys. D: Appl. Phys., **20**, No. 4. 444-452 (1987).
7. M. Hino, T. Aono, M. Nakajima, and S. Yuta, Appl. Opt., **25**, No. 22, 4742-4746 (1987).
8. A. T. Ramsey and S. L. Turner, Rev. Sci. Instrum., **58**, No. 7, 1211-1220 (1987).
9. Iokosha, Sasaki, Kawasima, et al., Prib. Nauch. Issled., No. 10, 93-96, (1988).

10. O. V. Filonin and G. B. Olelnikova, Prib. Tekh Éksp., No. 2, 230 (1989).
11. F. P. Press, Video Signal Shapers Based on Charge-Coupling Devices [Russian translation], Moscow (1981).
12. V. M. Efimov, A. M. Iskol'dskii, and Yu. E. Nesterikhin, Electron-Optical Photography in a Physical Experiment [in Russian], Novosibirsk (1978).
13. S. M. Slobodyan and T. N. Kitenko, Zarubezhnaya Radioélektronika, No. 7, 27-38 (1985).
14. A. N. Veklich and V. A. Zhovtyanskii, Zh. Prikl. Spektrosk., **50**, No. 4, 565-570 (1989).
15. L. I. Andreeva, V. A. Zhovtyanskii, S. A. Kaidalov, et al., Photoelectronic Instruments for Investigating High-Speed Processes [in Russian], Moscow (1979), pp. 97-108.
16. A. Ya. Smirnov and G. G. Men'shikov, Scanning Instruments [in Russian], Leningrad (1986).
17. V. P. Ivannikov, Élektron. Promyshlennost', No. 10 (178), 53-54 (1988).
18. P. M. Epperson, J. V. Sweedler, M. B. Denton, et al., Opt. Eng., **26**, No. 8, 715-723 (1987).
19. S. C. H. Wang, C. Y. Wei, H. H. Woodbury, et al., IEEE Trans. Electron Devices, **32**, 1599-1607 (1985).
20. G. D. Bakhtiarov, V. V. Malinin, and V. V. Shkolin, Analog–Digital Converters [in Russian], Moscow (1980).
21. F. P. Press, Electronics [in Russian], (Summaries of Science and Technology, VINITI)., Moscow (1986), Vol. 18, 38-88.
22. B. Rodericks. R. Clark, R. Smider, and A. Fontaine, Prib. Nauchn. Issled., No. 8. 11-16 (1989).
23. G. I. Aponin, A. A. Besshaposhnikov, and D. M. Kulakov, Prib. Tekh Éksp., No. 3, 173-174 (1986).
24. M. M. Blouke, D. L. Heidtmann, B. Corrle, and M. L. Lust, Proc. Soc. Photo-Opt. Instrum. Eng., **570**, 82-88 (1985).
25. I. A. Bez'yazynchnyi, E. F. Lifshits, A. K. Berezin, et al., Plasma Diagnostics [in Russian], Moscow (1973), No. 2, pp. 59-63.
26. L. I. Andreeva. V. S. Dobrolyubov, V. A. Zhovtyanskii, et al. Prib. Tekh. Éksp., No. 5, 267 (1979).
27. L. I. Andreeva, A. N. Veklich, A. P. Gulyi, et al., Prib. Tekh Éksp., No. 1, 241 (1987).
28. V. A. Zhovtyanskii, "Experimental investigation of a pulsed expanding plasma," Dissertation for Candidate of Physical-Mathematical Sciences, Kiev (1985).
29. V. A. Zhovtyanskii, K. V. Nelep, and O. M. Novik, Zh. Prikl. Spektrosk., **49**, No. 3, 400-407 (1988).
30. V. A. Zhovtyanskii and O. M. Novik, Zh. Tekh. Fiz., **59**, No. 9, 186-189 (1989).
31. I. L. Babich, A. N. Veklich, and V. A. Zhovtyanskii, Zh. Prikl. Spektrosk.. **51**, No. 4, 571-575 (1989).
32. R. F. Harber and G. E. Sonnek, Appl. Opt., **5**, No. 6, 1039-1043 (1966).
33. E. N. Eberhardt and R. J. Hertel, Appl. Opt., **10**, No. 8, 1972-1974 (1971).
34. P. G. Weber, Rev. Sci. Instrum., **54**, No. 10, 1331-1333 (1983).
35. P. Lindblom, S. Engman, A. Danielson, and E. Soderman, Phys. Scr., **22**, No. 1, 61-67 (1980).
36. A. Danielson and L. Lindblom, Appl. Spectrosc., **30**, No. 2, 151-155 (1976).